

1 **Inarticulate past: Similarity properties of the ice-climate system and their implications for paleo-**  
2 **records attribution**

3 *Mikhail Y. Verbitsky*

4 Gen5 Group, LLC, Newton, MA, USA  
5 UCLouvain, Earth and Life Institute, Louvain-la-Neuve, Belgium  
6 Correspondence: Mikhail Verbitsky (verbitskys@gmail.com)  
7

8 **Abstract.** Reconstruction and explanation of past climate evolution using proxy records is the essence of  
9 paleoclimatology. In this study, we use dimensional analysis of a dynamical model on orbital time-scales to  
10 recognize theoretical limits of such forensic inquiries. Specifically, we demonstrate that major past events could  
11 have been produced by physically unsimilar processes making the task of paleo-records attribution to a particular  
12 phenomenon to be fundamentally difficult, if not impossible. It also means that any future scenario may not have a  
13 unique cause and, in this sense, the orbital time-scale future may be to some extent less sensitive to specific  
14 terrestrial circumstances.  
15

16 **Introduction**

17  
18 Interpretation of most prominent events of climate history such as the middle-Pleistocene transition  
19 (Ruddiman et al., 1986, Lisiecki and Raymo, 2005, Clark et al., 2021) has been an inspiration for several generations  
20 of climate modelers (see for a review Saltzman, 2002, Tziperman et al., 2006, Crucifix, 2013, Mitsui and Aihara,  
21 2014, Paillard, 2015, Ashwin and Ditlevsen, 2015, Verbitsky et al, 2018, Willeit et al., 2019, Riechers et al, 2022).  
22 While specific physical mechanisms invoked to explain changing glacial rhythmicity vary, they all include slow  
23 changes of ocean-atmosphere governing parameters (e.g., Saltzman and Verbitsky, 1993; Raymo, 1997; Paillard and  
24 Parrenin, 2004) or glaciation parameters (Clark and Pollard, 1998). On a more general level, all these theories in fact  
25 assume slow changes in the intensities of positive (such as, for example, long-term variations in carbon dioxide  
26 concentration, e.g., Saltzman and Verbitsky, 1993) or negative (for example, regolith erosion, Clark and Pollard,  
27 1998, or diminished role of the geothermal heat flux relative to the vertical temperature advection in growing ice  
28 sheets, Verbitsky and Crucifix, 2021) system feedbacks. Though all physical phenomena invoked are, indeed, real  
29 and may be plausible, the following question still remains unanswered: Is it possible to disambiguate the past and  
30 elevate a single “correct” theory? Answering this question is the goal of our study.

31 Indeed, this is the classical attribution challenge that has been successfully addressed in the context of another  
32 well-known problem of geophysics: the causality of the observed global warming. For this purpose, the most  
33 comprehensive space-resolving models have been employed to reproduce observed time-series under different  
34 conditions and to prove (or discredit) a candidate physical phenomenon (e.g., Stocker, 2014). Certainly, these  
35 models cannot be employed on extremely long orbital time-scales (10 – 100 kyr) due to computational constrains. In  
36 search for an alternative, we turn here to dimensional analysis. Historically, dimensional analysis and concepts of  
37 similarity have been used for studying physical phenomena, complementing even the most sophisticated  
38 computational tools and providing physical insight in situations where physical interpretation of the higher-  
39 complexity modeling results may be difficult. Here, on orbital timescales, when we retreat from physics-abundant  
40 space-resolving models to more conceptual dynamical models, dimensional analysis may be promoted from a  
41 supporting to a more prominent role.

42 Several key terms need to be introduced before we outline the structure of our paper. We will be using the  
43 definitions of similarities as they have been articulated by G. I. Barenblatt (2003). Suppose we have a physical  
44 phenomenon that is governed by  $n$  physical parameters,  $k$  parameters of which are parameters with independent  
45 dimensions. Then, according to  $\pi$ -theorem (Buckingham, 1914), the phenomenon can be described by  $n-k$   
46 adimensional similarity parameters  $\pi_1, \pi_2, \dots, \pi_i, \dots, \pi_{n-k}$ . We will consider two phenomena as being *physically*  
47 *similar* if they are described by identical similarity parameters  $\pi_1, \pi_2, \dots, \pi_i, \dots, \pi_{n-k}$ . The dimensionless time series  
48 of physically similar processes are also identical. If a similarity parameter  $\pi_i$  can be excluded from the description of  
49 a physical process (a phenomenon becomes independent of it in the limit that  $\pi_i$  tends to zero or infinity) we can talk  
50 about *complete similarity* of this physical process in this parameter: regardless of parameter’s specific value, the  
51 process does not depend on it. And, finally, we may observe *incomplete similarity* when none of similarity  
52 parameters  $\pi_1, \pi_2, \dots, \pi_i, \dots, \pi_{n-k}$  can be neglected even if they are too small (or too big), but the number of effective

53 parameters may still be reduced because a phenomenon depends not on actual values of similarity parameters but on  
 54 their products in some power degree (i.e., conglomerate similarity groups):

55  $\Pi_j = (\pi_1^{\alpha_j}) (\pi_2^{\beta_j}) \dots (\pi_l^{\lambda_j}) \dots (\pi_{n-k}^{\chi_j})$  ( $j = 1, 2, \dots, l; l < n - k$ ). Here  $\alpha_j, \beta_j, \dots, \lambda_j, \dots, \chi_j$  are power degrees  
 56 of  $\pi_1, \pi_2, \dots, \pi_l, \dots, \pi_{n-k}$  involved into  $\Pi_j$  formulation.

57 We are now ready to proceed with the structure of our paper: (a) first, we will introduce our dynamical  
 58 model and describe major physical processes involved; (b) using dimensional analysis, we will define 8 similarity  
 59 parameters  $\pi_1 - \pi_8$  that completely define model's behavior; (c) Since our system does not have a property of  
 60 complete similarity in any of individual parameters  $\pi_1 - \pi_8$ , we will attempt to discover incomplete similarity and  
 61 find conglomerate similarity groups. Unfortunately, there are no specific algorithms that can help us to determine  
 62 governing conglomerate similarity groups  $\Pi_j$ , if they indeed exist. Therefore, we will articulate such conglomerate  
 63 similarity groups based on observed system behavior; (d) we will then discuss implications of our findings for the  
 64 attribution challenge and illustrate our reasoning with a numerical experiment; (e) we will conclude our study with  
 65 some thoughts relating our results to the real-world climate system.

## 67 Method

68  
 69 For our experiments we employ the Verbitsky et al (2018), VCV18 thereafter, dynamical model of the ice-  
 70 climate system. It has been derived from the scaled mass- and heat-balance equations of the non-Newtonian ice  
 71 flow, i.e., equations (1) and (2), correspondingly, and combined with an energy-balance equation of the global  
 72 climate temperature (3):

$$73 \frac{dS}{dt} = \frac{4}{5} \zeta^{-1} S^{3/4} (a - \varepsilon F_S - \kappa \omega - c \theta) \quad (1)$$

$$74 \frac{d\theta}{dt} = \zeta^{-1} S^{-1/4} (a - \varepsilon F_S - \kappa \omega) \{ \alpha \omega + \beta [S - S_0] - \theta \} \quad (2)$$

$$75 \frac{d\omega}{dt} = -\gamma [S - S_0] - \frac{\omega}{\tau} \quad (3)$$

76  
 77 Here,  $S$  ( $\text{m}^2$ ) is the area of glaciation,  $\theta$  ( $^\circ\text{C}$ ) is the basal ice-sheet temperature, and  $\omega$  ( $^\circ\text{C}$ ) is the global temperature  
 78 of the ocean-atmosphere (rest of the climate) system. In deriving equations (1) and (2) we consider ice sheets in the  
 79 thin-boundary-layer approximation such that their inertial forces are negligible relative to stress gradients, and  
 80 motion equations with very high accuracy can be written in a quasi-static form. For such approximation, a  
 81 characteristic ice thickness  $H$  is connected to ice area  $S$  as  $H = \zeta S^{1/4}$  where  $\zeta$  ( $\text{m}^{1/2}$ ) is a profile factor assumed to  
 82 be constant (Verbitsky and Chalikov, 1986, VCV18). Further, equation (1) represents global ice balance  $\frac{d(HS)}{dt} =$   
 83  $AS$ , where, again,  $H = \zeta S^{1/4}$  and  $A = a - \varepsilon F_S - \kappa \omega - c \theta$  is the surface mass influx. Equation (2) describes  
 84 vertical ice temperature advection with a time scale  $H/(a - \varepsilon F_S - \kappa \omega)$ , and equation (3) is the global energy-  
 85 balance equation. The parameter  $a$  ( $\text{m s}^{-1}$ ) is the snow precipitation rate;  $F_S$  is normalized external forcing,  
 86 specifically, mid-July insolation at  $65^\circ\text{N}$  (Berger and Loutre, 1991) of the amplitude  $\varepsilon$  ( $\text{m s}^{-1}$ ) such that  $\varepsilon F_S$  describes  
 87 ice ablation rate due to astronomical forcing;  $\kappa \omega$  is the ice ablation rate representing the cumulative effect of the  
 88 global climate on ice-sheet mass balance;  $c \theta$  represents ice discharge due to ice-sheet basal sliding;  $\alpha \omega$  is basal  
 89 temperature response to global climate temperature change,  $\beta [S - S_0]$  is basal temperature reaction to the changes  
 90 of ice geometry;  $-\gamma [S - S_0]$  describes global temperature response to ice geometry changes (e.g., albedo);  $\kappa$  ( $\text{m s}^{-1}$   
 91  $^\circ\text{C}^{-1}$ ),  $c$  ( $\text{m s}^{-1} \text{ }^\circ\text{C}^{-1}$ ),  $\alpha$  (adimensional),  $\beta$  ( $^\circ\text{C m}^{-2}$ ) and  $\gamma$  ( $^\circ\text{C m}^{-2} \text{ s}^{-1}$ ) are sensitivity coefficients;  $S_0$  ( $\text{m}^2$ ) is a reference  
 92 glaciation area; and  $\tau$  (s) is the timescale for  $\omega$ . When orbitally forced, the model reproduced events of the last  
 93 million years reasonably well, except for the interglacial of 400 kyr ago (marine isotopic stage 11). The timing of all  
 94 other interglacials coincides with Past Interglacial Working Group of PAGES (2016) data (VCV18).

95 We will now focus on the most remarkable feature of the historical records - a period  $P$  of climate response  
 96 to the astronomical forcing. Indeed, it is the change of the climate variability from the predominant period  $P = 40$   
 97 kyr to the main periods of  $P = 80$ -120 kyr that makes the middle-Pleistocene transition so extraordinary. Though the  
 98 amplitude increase was considered, until recently, to be a necessary attribute of this transition, its presence in the  
 99 paleo-records is now questioned (Clark et al, 2021). We begin with the dimensional analysis of the VCV18 system  
 100 (1) – (3). Indeed, it has 11 governing parameters (including the amplitude  $\varepsilon$  and the period  $T$  of the external forcing).  
 101 If we choose  $\varepsilon$ ,  $T$  and  $\gamma$  to be parameters with independent dimensions, then in accordance with  $\pi$ -theorem a period  
 102 of the system response can be fully described by 8 dimensionless similarity parameters  $\pi_1 - \pi_8$ :

103

$$104 \quad \pi_1 = \frac{\varepsilon}{a}, \pi_2 = \alpha, \pi_3 = \kappa\gamma\varepsilon T^3, \pi_4 = c\gamma\varepsilon T^3, \pi_5 = \frac{T}{\tau}, \pi_6 = \frac{\gamma T}{\beta}, \pi_7 = \frac{S_0}{\varepsilon^2 T^2}, \pi_8 = \frac{\varsigma}{\varepsilon^{1/2} T^{1/2}}, \text{ and}$$

105

$$106 \quad P = T\Psi(\pi_1, \pi_2, \dots, \pi_8) \quad (4)$$

107

108 The numerical experiments with the system (1) – (3) demonstrate that individual similarity parameters  $\pi_1 - \pi_8$   
 109 cannot be discarded using simply “too big” or “too small” arguments. It means that the system (1) – (3) does not  
 110 have a property of complete similarity in any of individual parameters  $\pi_1 - \pi_8$ . At the same time, we observed  
 111 earlier (Verbitsky and Crucifix, 2020) that the period of the system (1) – (3) response to the obliquity forcing of  
 112 period  $T$  is mostly governed by two dimensionless parameters: by the ratio of the astronomical forcing amplitude to  
 113 terrestrial ice sheet snow precipitation rate,  $\varepsilon/a$ , and by the adimensional  $V$ -number. The physical meaning of the  $V$ -  
 114 number in the orbital domain becomes most evident if we take a closer look into the structure of positive and  
 115 negative feedbacks as they appear in the system (1) – (3). The time-dependent negative feedback is proportional to  
 116 the ice sheet area size as  $\beta(S - S_0)$ . The coefficient  $\beta$  is defined by thermodynamical properties of an ice sheet,  
 117 most importantly by the Peclet number,  $Pe = \hat{A}H/k$ ,  $\hat{A}$  is a characteristic mass influx, i.e., accumulation minus  
 118 ablation and  $k$  is ice temperature diffusivity (VCV18, Verbitsky and Crucifix, 2021). This negative feedback acts on  
 119 ice-sheet mass balance with a vertical-advection time delay and is amplified by a sensitivity coefficient  $c$  that  
 120 reflects the intensity of basal sliding. The time-dependent positive feedback is global temperature  $\omega$ . In the orbital  
 121 domain,  $\tau \ll T$  ( $\pi_5 \gg 1$ ),  $\omega$  is approximately proportional to  $-\gamma\tau(S - S_0)$ . The global temperature acts on the ice-  
 122 sheet mass balance “instantly” as  $\kappa\omega$  and with the vertical-advection time-delay as a component of basal temperature  
 123 conditions,  $a\omega c$ . Thus, the  $V$ -number is emerging in the orbital domain as a ratio of amplitudes of time-dependent  
 124 positive and negative feedbacks.

125

$$126 \quad V = \frac{\gamma\tau}{\beta c}(\alpha c + \kappa) \quad (5)$$

127

128 Specifically, when  $V \sim 0.75$  and  $\varepsilon/a \sim 1$ , the system exhibits the obliquity-period doubling. When the positive  
 129 feedback and the obliquity forcing are less articulated, the system responds with the 40-kyr period. Thus, slow  
 130 changes of the  $V$ -number (for example, from  $V = 0.5$  at  $t = 3,000$  kyr ago to  $V = 0.75$  at  $t = 0$ ) and of the  $\varepsilon/a$  ratio (for  
 131 example, from  $\varepsilon/a = 0.3$  to  $\varepsilon/a = 1.7$  over the same time span) produce a change in the ice-climate behavior similar  
 132 to the middle-Pleistocene transition.

133 We now notice that the  $V$ -number can be presented in terms of similarity parameters  $\pi_1 - \pi_8$ , specifically:

134

$$135 \quad V = \frac{\gamma\tau}{\beta c}(\alpha c + \kappa) = \left(\pi_2 + \frac{\pi_3}{\pi_4}\right) \frac{\pi_6}{\pi_5} \quad (6)$$

136

137 We also experimentally established that the period-doubling sustains ( $\Psi = 2$ ) if, under fixed  $\varepsilon/a$  and  $V$ , the period  
 138 of the external forcing changes from let say  $T = 35$  kyr to  $T = 50$  kyr. It can only happen if in this domain similarity  
 139 parameters  $\pi_7$  and  $\pi_8$  make another conglomerate similarity group that does not depend on  $T$ , specifically  $\frac{\pi_8^4}{\pi_7}$ .

140 Thus, equation (4) can be written as

141

$$142 \quad P = T\Psi\left(\pi_1, \frac{\pi_2\pi_6}{\pi_5}, \frac{\pi_3\pi_6}{\pi_4\pi_5}, \frac{\pi_8^4}{\pi_7}\right), \quad (7)$$

143

144 that is the pure case of incomplete similarity as we defined it above: none of the similarity parameters can be  
 145 neglected but instead of 8 governing parameters we have been able to migrate to 4 governing conglomerate

146 similarity groups. Finally we may notice that  $\frac{\pi_8^4}{\pi_7} = \frac{H^4}{S_0^2} \ll 1$  for all large ice sheets. If, we set it to be constant, we

147 can re-write equation (7) in a more simple form as

148

$$149 \quad P = T\Psi\left(\frac{\varepsilon}{a}, V\right) \quad (8)$$

150

151 Recognition of governing conglomerate similarity groups is important because it provides us with a powerful  
 152 insight: different combinations of similarity parameters  $\pi_i$  may produce the same  $V$ -number, i.e., *physically*

153 *unsimilar processes* (formed by not identical  $\pi_i$ ) *may cause the same outcome*. This observation is critical for our  
154 attribution challenge. Certainly, precise disambiguation of historical records is always a difficult task because even  
155 two physically similar processes having identical adimensional similarity parameters and demonstrating the same  
156 behavior may have been produced by different values of physical parameters involved, unless these parameters are  
157 physical constants or well defined. The situation becomes especially challenging when we deal with conglomerate  
158 similarity groups because, as we just stated, the same results may be produced by not-identical similarity parameters  
159 (physically unsimilar processes). This is the theoretical limit that we aspire to expose.

160 We will now apply our findings to the middle-Pleistocene transition. Since the physical interpretation of the  
161 governing parameters incorporated in the conglomerate  $V$ -number is very straightforward, we may observe a similar  
162 (in terms of the period- $P$  bifurcation) system response to changes of a completely different physical nature. For  
163 example, parameter  $\beta$ , as we have discussed above, defines intensity of the negative feedback and is formed as a  
164 result of interplay between vertical ice advection, internal friction, and geothermal heat flux (VCV18). Increased  
165 Peclet number of growing ice sheet diminishes the role of the geothermal heat flux and may reduce parameter  $\beta$  thus  
166 increasing the  $V$ -number. The same period- $P$  bifurcation can also be caused, for example, by slow changes in the  
167 parameter  $\gamma$  that defines the intensity of the positive feedback and incorporates effects of the albedo change or other  
168 atmospheric feedbacks. We solve equations (1) – (3) for these two cases. In both cases we invoke a global cooling  
169 trend. In our first experiment (Fig. 1a), this trend is translated into reduction of  $\beta$ , i.e., weakening of the ice sheet  
170 negative feedback, and corresponding increase of the  $V$ -number from  $V = 0.5$  to  $V = 0.75$ . The increased  
171 continentality of the climate (reduced intensity of the snowfall during colder climate) is accounted by the  $\varepsilon/a$  ratio  
172 increase from  $\varepsilon/a = 0.3$  to  $\varepsilon/a = 1.7$ . In the second experiment (Fig. 1b), the  $V$ -number also evolves from  $V = 0.5$  to  $V$   
173  $= 0.75$ , but this time it is achieved by increased intensity of the positive feedback ( $\gamma$ ). In both experiments, we used  
174 mid-July insolation at  $65^\circ\text{N}$  (Berger and Loutre, 1991) for the last 3 million years as an astronomical forcing. The  
175 millennial forcing is added to  $\varepsilon F_5$  as a single sinusoid of 5 kyr period and doubled ( $2\varepsilon$ ) amplitude. It is important to  
176 note that in the first experiment (changing  $a$  and  $\beta$ ) only similarity parameters  $\pi_1$  and  $\pi_6$  are being changed, but in  
177 the second experiment (changing  $a$  and  $\gamma$ ) the same changes of the  $V$ -number are caused by changing  $\pi_1, \pi_3, \pi_4, \pi_6$ .  
178 It means that the processes involved in these two experiments are not physically similar. Though the time-series  
179 produced in these two cases are obviously non-identical (see Fig. 1 inserts), we can observe that different physical  
180 phenomena may produce the same changes in the conglomerate  $V$ -number and the same large-scale effect, i.e., the  
181 period-doubling bifurcation at about 1 Myr ago.

182 We do not attempt here to fully reproduce paleo-records such as the Lisiecki and Raymo (2005) and a  
183 discussion of whether a period doubling should be accompanied by the amplitude increase is outside of the current  
184 paper's scope. We will just remark that the amplitude of the system response is the function of not just the period  $P$   
185 but also of the  $\varepsilon/a$  ratio (Verbitsky and Crucifix, 2020) and, for example, less articulated continentality of colder  
186 climates may explain diminished amplitude contrasts as it has been recently advocated by Clark et al (2021).

187 Indeed, as we have already indicated, we used mid-July insolation at  $65^\circ\text{N}$  for the last 3 million years as an  
188 astronomical forcing. Apart from that, these examples may also serve as an illustration of some future scenarios of  
189 the climate system behavior under post-industrial atmospheric carbon dioxide concentration reduction as implied by  
190 Ridgwell and Hargreaves (2007). Again, regardless of the physical nature of the underlying dynamical system, it  
191 exhibits 40-kyr rhythmicity of the first 1.5 million years of its evolution and consequent obliquity-period doubling.  
192 This probable renaissance of ice-ages is different from the one envisioned by Talento and Ganapolski (2021) which  
193 is based on the model tuned to the late Pleistocene (last 800 kyr) ice-volume data and thus postulates only 100-kyr-  
194 period variability for the future.

## 195 **Conclusions**

197 The idea of the current presentation is simple but its implication may be important: If ice-climate system is defined  
198 by conglomerate similarity groups, then we may be limited in our ability to disambiguate historical records and  
199 different physical processes may produce same future scenarios. The latter is intriguing because since B. Saltzman  
200 (1962) and E. Lorenz (1963) had discovered a hydrodynamic system's sensitivity to initial conditions, the concept of  
201 deterministic chaos became a dominant concept of weather and climate theory. Our findings suggest that if we  
202 consider orbital time scales and, instead of time series, focus on their more generalized attributes such as the period  
203 of the system response to the astronomical forcing, we may observe that the behavior of these attributes may be, to  
204 some extent, less sensitive to the physical nature of the terrestrial governing processes.

205 But do conglomerate similarity groups indeed govern the dynamics of the real orbital-scale climate system?  
206 So far, these groups have been found only in our VCV18 low-order dynamical model, and although this model has  
207 been explicitly derived from the conservation laws, our concept will remain hypothetical until it is supported by

208 empirical data. We speculate, though, that existing historical records may perhaps provide some support to our  
209 theory. To evaluate the feasibility of a diagnostic approach, we entertain here a simple scaling exercise. Suppose  
210 that an empirical time series, such as  $\delta^{18}\text{O}$  record, is created by a parent system (other than the VCV18) which is  
211 controlled by  $n$  physical parameters ( $k$  of them having independent dimensions). If we choose the period of the  
212 astronomical forcing  $T$  to be among parameters with independent dimensions, then in accordance with the  $\pi$ -theorem  
213 we have:

$$214 \quad P = T\Psi(\pi_1, \pi_2, \dots, \pi_{n-k}) \quad (9)$$

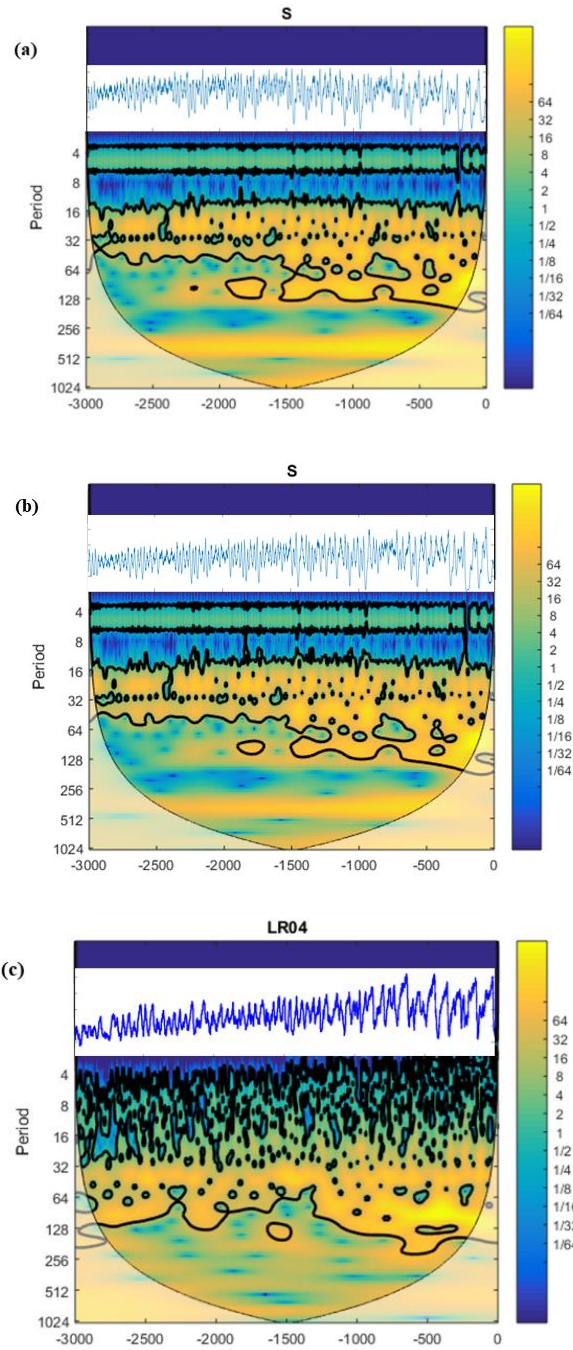
216 The wavelet spectrum of the late Pleistocene  $\delta^{18}\text{O}$  variability in response to the precession ( $\sim 20$ -kyr period) and  
217 obliquity ( $\sim 40$ -kyr period) forcing shows the dominance of 40-kyr and 80-kyr periods (Fig. 1c). If we are willing to  
218 accept it as a hint of  $\Psi = 2$  for  $T = 20$  kyr and for  $T = 40$  kyr, then, since some of the similarity parameters  
219  $\pi_1, \pi_2, \dots, \pi_{n-k}$  depend on  $T$ , the period- $T$  independence of  $\Psi$  may only happen when  $\pi_1, \pi_2, \dots, \pi_{n-k}$  make  
220 conglomerate  $T$ -independent groups. In other words, *period independence of the  $\Psi$  function may be a fingerprint of*  
221 *conglomerate similarity groups*. Indeed, the diagnostics of the  $\Psi$  function may require much more sophisticated  
222 instruments than our *ad hoc* reasoning, and the records will likely not explicitly reveal what the conglomerate  
223 similarity groups look like; nevertheless, their mere existence would corroborate the idea of this paper.  
224

225  
226 **Competing interests:** The author declares that he has no conflict of interest.  
227 **Acknowledgements:** The author is grateful to Michel Crucifix for multiple discussions related to this topic and to  
228 Jeremy Bassis and anonymous reviewer for their helpful comments.  
229

## 230 References

- 231 Ashwin, P. and Ditlevsen, P.: The middle Pleistocene transition as a generic bifurcation on a slow manifold, *Clim.*  
232 *Dynam.*, 45, 2683–2695, <https://doi.org/10.1007/s00382-015-2501-9>, 2015.  
233  
234 Barenblatt, G. I.: *Scaling*, Cambridge University Press, Cambridge, 2003.  
235  
236 Berger, A. and Loutre, M. F.: Insolation values for the climate of the last 10 million years, *Quaternary Sci. Rev.*, 10,  
237 297–317, 1991.  
238  
239 Buckingham, E.: On physically similar systems; illustrations of the use of dimensional equations, *Phys. Rev.*, 4,  
240 345–376, 1914.  
241  
242 Clark, P. U. and Pollard, D.: Origin of the middle Pleistocene transition by ice sheet erosion of regolith,  
243 *Paleoceanography*, 13, 1–9, 1998.  
244  
245 Clark, P. U., Shakun, J., Rosenthal, Y., Köhler, P., Schrag, D., Pollard, D., Liu, Z., and Bartlein, P.: Requiem for the  
246 Regolith Hypothesis: Sea-Level and Temperature Reconstructions Provide a New Template for the Middle  
247 Pleistocene Transition. No. EGU21-13981. Copernicus Meetings, 2021.  
248  
249 Crucifix, M.: Why could ice ages be unpredictable?, *Clim. Past*, 9, 2253–2267, [https://doi.org/10.5194/cp-9-2253-](https://doi.org/10.5194/cp-9-2253-2013)  
250 [2013](https://doi.org/10.5194/cp-9-2253-2013), 2013.  
251  
252 Lisiecki, L. E. and Raymo, M. E.: A Pliocene-Pleistocene stack of 57 globally distributed benthic  $\delta^{18}\text{O}$  records,  
253 *Paleoceanography*, 20, PA1003, <https://doi.org/10.1029/2004PA001071>, 2005.  
254  
255 Lorenz, E.N.: Deterministic nonperiodic flow, *Journal of atmospheric sciences*, 20, 2, 130-141, 1963.  
256  
257 Mitsui, T. and Aihara, K.: Dynamics between order and chaos in conceptual models of glacial cycles, *Clim. Dynam.*,  
258 42, 3087–3099, 2014.  
259  
260 Paillard, D.: Quaternary glaciations: from observations to theories, *Quaternary Sci. Rev.*, 107, 11–24,  
261 <https://doi.org/10.1016/j.quascirev.2014.10.002>, 2015.

262  
263 Paillard, D. and Parrenin, F.: The Antarctic ice sheet and the triggering of deglaciations, *Earth Planet. Sc. Lett.*, 227,  
264 263–271, 2004.  
265  
266 Past Interglacial Working Group of PAGES: Interglacials of the last 800,000 years, *Rev. Geophys.*, 54, 162–219,  
267 2016.  
268  
269 Raymo, M.: The timing of major climate terminations, *Paleoceanography*, 12, 577–585,  
270 <https://doi.org/10.1029/97PA01169>, 1997.  
271  
272 Ridgwell, A., and Hargreaves, J. C.: Regulation of atmospheric CO<sub>2</sub> by deep-sea sediments in an Earth system  
273 model. *Global Biogeochemical Cycles* 21, no. 2, <https://doi.org/10.1029/2006GB002764>, 2007.  
274  
275 Riechers, K., Mitsui, T., Boers, N., and Ghil, M.: Orbital insolation variations, intrinsic climate variability, and  
276 Quaternary glaciations, *Clim. Past*, 18, 863–893, <https://doi.org/10.5194/cp-18-863-2022>, 2022.  
277  
278 Ruddiman, W. F., Raymo, M., and McIntyre, A.: Matuyama 41,000-year cycles: North Atlantic Ocean and northern  
279 hemisphere ice sheets, *Earth Planet, Sc, Lett.*, 80, 117–129, [https://doi.org/10.1016/0012-821X\(86\)90024-5](https://doi.org/10.1016/0012-821X(86)90024-5), 1986.  
280  
281 Saltzman, B.: Finite amplitude free convection as an initial value problem—I, *Journal of atmospheric sciences*, 19,  
282 4, 329-341, 1962.  
283  
284 Saltzman, B.: Dynamical paleoclimatology: generalized theory of global climate change, in: Vol. 80, Academic  
285 Press, San Diego, CA, 2002.  
286  
287 Saltzman, B. and Verbitsky, M. Y.: Multiple instabilities and modes of glacial rhythmicity in the Plio-Pleistocene: a  
288 general theory of late Cenozoic climatic change, *Clim. Dynam.*, 9, 1–15, 1993.  
289  
290 Stocker, T. (Ed.): *Climate change 2013: the physical science basis: Working Group I contribution to the Fifth*  
291 *assessment report of the Intergovernmental Panel on Climate Change*, Cambridge University Press, Chapter 10:  
292 *Detection and Attribution of Climate Change: from Global to Regional*, 867–952, 2014.  
293  
294 Talento, S. and Ganopolski, A.: Reduced-complexity model for the impact of anthropogenic CO<sub>2</sub> emissions on  
295 future glacial cycles, *Earth Syst. Dynam.*, 12, 1275–1293, <https://doi.org/10.5194/esd-12-1275-2021>, 2021.  
296  
297 Tziperman, E., Raymo, M. E., Huybers, P., and Wunsch, C.: Consequences of pacing the Pleistocene 100 kyr ice  
298 ages by nonlinear phase locking to Milankovitch forcing, *Paleoceanography*, 21, PA4206,  
299 <https://doi.org/10.1029/2005PA001241>, 2006.  
300  
301 Verbitsky, M. Y. and Chalikov, D. V.: *Modelling of the Glaciers-Ocean-Atmosphere System*, Gidrometeoizdat,  
302 Leningrad, 1986.  
303  
304 Verbitsky, M. Y. and Crucifix, M.:  $\pi$ -theorem generalization of the ice-age theory, *Earth Syst. Dynam.*, 11, 281–  
305 289, <https://doi.org/10.5194/esd-11-281-2020>, 2020.  
306  
307 Verbitsky, M. Y. and Crucifix, M.: ESD Ideas: The Peclet number is a cornerstone of the orbital and millennial  
308 Pleistocene variability, *Earth Syst. Dynam.*, 12, 63–67, <https://doi.org/10.5194/esd-12-63-2021>, 2021.  
309  
310 Verbitsky, M. Y., Crucifix, M., and Volobuev, D. M.: A theory of Pleistocene glacial rhythmicity, *Earth Syst.*  
311 *Dynam.*, 9, 1025–1043, <https://doi.org/10.5194/esd-9-1025-2018>, 2018.  
312  
313 Willeit, M., Ganopolski, A., Calov, A., and Brovkin, V.: Mid-Pleistocene transition in glacial cycles explained by  
314 declining CO<sub>2</sub> and regolith removal, *Science Advances* 5, 4, <https://www.science.org/doi/10.1126/sciadv.aav7337>,  
315 2019



316 **Fig. 1** Ice-climate system response to a cooling trend presented as an evolution of wavelet spectra over 3 Myr for  
 317 calculated ice-sheet glaciation area  $S$  ( $10^6 \text{ km}^2$ ) – panels (a) and (b), and for the Lisiecki and Raymo (2005) benthic  
 318  $\delta^{18}\text{O}$  record, panel (c). The  $V$ -number evolves from  $V = 0.5$  to  $V = 0.75$  due to weakening of the negative feedback  
 319 (a) and due to intensified positive feedback (b). The vertical axis is the period (kyr), the horizontal axis is time (kyr  
 320 before present). The color scale shows the continuous Morlet wavelet amplitude, the thick line indicates the peaks  
 321 with 95 % confidence, and the shaded area indicates the cone of influence for wavelet transform. Inserts are  
 322 corresponding time series.